Formation, Composition and Evolution of the Earth's Core

Francis Nimmo, University of California Santa Cruz

Summary

The Earth's core formed by multiple collisions with differentiated proto-planets. The Hf-W isotopic system reveals that these collisions took place over a timescale of tens of Mega-years (Myr), in agreement with accretion simulations. The degree to which the iron and silicates re-equilibrated during each collision is uncertain, and affects the apparent core age derived from tungsten isotopic measurements. Seismological data reveal that the core contains light elements in addition to Fe-Ni, and the outer core is more enriched in such elements than the inner core. Because O is excluded efficiently from solid iron, O is almost certainly an important constituent of the outer core. The identity of other elements is less certain, despite intensive measurements of their effects on seismic velocities, densities and partitioning behavior at appropriate pressures and temperatures. Si and O are very likely present, with perhaps some S; C and H are less likely. Si and Mg may have exsolved over time, potentially helping to drive the geodynamo and producing a low density layer at the top of the core. Radioactive elements (U,Th,K) are unlikely to be present in important concentrations. The cooling of the core is controlled by the mantle's ability to extract heat. The geodynamo has existed for at least 3.5 Gyr, placing a lower bound on the heat flow out of the core. Because the thermal conductivity of the core is uncertain by a factor of ~3, the lower bound on this heat flow is similarly uncertain. Once the inner core started to crystallize, additional sources of energy were available to power the geodynamo. Inner core crystallization likely started in the time range 0.5-2.0 Gyr before present (B.P.); paleomagnetic arguments have been advanced for inner core growth starting at several different epochs within this time range.

Keywords: Core, element partitioning, planetary accretion, geodynamo, light element, inner core

1. Introduction

The Earth's core is a sphere of molten iron, 3480 km in radius, containing a smaller solid inner core 1220 km in radius. It is important for at least three reasons: it provides clues to the manner and timing of Earth's formation; the existence of an inner core tells us about the long-term thermal evolution of the Earth; and the Earth's magnetic field originates within the vigorously-convecting outer core. Furthermore, iron cores are a universal feature among the inner rocky planets, and at least some satellites (e.g. Io, Ganymede); an improved understanding of the Earth's core helps us understand the cores of these less well-characterized planetary bodies.

The gross structure of the core has been known since the 1940s from seismological studies; more recently, attention has been focused on its formation, composition and evolution, and these topics are the focus of this article. The formation of the Earth, and that of the core itself, is addressed first. Conditions during core formation were important in establishing the composition of the core, which is the subject of the second section of this article. Finally, the initial thermal and compositional conditions set by core formation will have affected its long-term evolution and its attendant magnetic field, which is the subject of the last section.

Many recent reviews cover these topics in more detail than is possible here: on core formation, good starting points include Rubie et al. (2015a) and Nimmo & Kleine (2015); on core composition and evolution, Hirose et al. (2013) and Litasov & Shatskiy (2016) are useful. A longer list of overview papers can be found at the end of this article.

2. Formation

2.1 How did the Earth form?

The early solar system was a swirling disk of dust and gas. The dust particles collided and, by poorly-understood processes and over perhaps 0.1 Myr, built asteroid-sized objects known as planetesimals. The bulk compositions of these objects reflected that of the initial solar nebula, a composition that is still recorded in some meteorites (the so-called CI chondrites). Continued collisions built Mars-mass "embryos" by a few Myr, and finally embryo-embryo collisions built the Earth.

This conventional picture of accretion derives in part from cosmochemical and isotopic measurements, but also from dynamical simulations in which the later stages of planetary accretion can be modeled by tracking swarms of orbiting particles in a computer (e.g. Raymond et al. 2006, O'Brien et al. 2014). The accretion timescales produced by these N-body models agree remarkably well with isotopic chronometers (see Sec 2.3). The models also show that "giant" collisions, of embryos with protoplanets, are an inescapable part of accretion. Such impacts are thought to be responsible for the formation of the Earth's Moon, and the loss of most of Mercury's mantle (e.g. Asphaug 2010).

In the last few years, two modifications to the conventional N-body story have been proposed. The first is that Jupiter and Saturn, rather than remaining static, migrated a significant distance towards the Sun, and then back out again, considerably changing the accretion dynamics (Walsh et al. 2011). This suggestion, the so-called "Grand Tack", certainly has effects on accretion timescales and the violence of collisions, but is not fundamentally different to the conventional picture.

The other proposal is more fundamental. It posits that much of accretion took the form of decimeter-scale "pebbles" accreting onto embryos (e.g. Bitsch et al. 2015). Accretion by this route can be rapid enough to allow even a distant body to grow large enough to retain hydrogen before the nebula disperses, and thus grow into a gas giant planet. Pebble accretion alone certainly cannot explain characteristics of the inner solar system planets (e.g. the formation of the Moon). However, it might be a viable mechanism for the early growth of embryos, before the more conventional late-stage accretion processes take over. Further work on this topic is required.

2.1.1 Thermal state of growing bodies

The thermal (and hence mechanical) state of the growing bodies was important in determining how core formation happened. Neglecting tides, there are only two important sources of energy available to heat planetary interiors: gravitational energy; and radioactive decay.

Gravitational energy heats a planet because a large fraction of the kinetic energy of impacting bodies is ultimately dissipated as heat. If the impactor is small, the heat is deposited in the near-surface and will be efficiently radiated to space unless accretion is very rapid. However, a large impactor will deposit most of its heat at depth, so the heat is retained. A back-of-the-envelope calculation in which all gravitational energy of an accreting body is converted to heat yields the temperature change ΔT due to accretion: $\Delta T = 3GM / 5RC_p$=35,000 K $(M/M_E)^{2/3}$ (e.g. Rubie et al. 2015a). Here M is the mass of the final planet, R is its radius, M_E is the mass of the Earth and C_p is the bulk specific heat capacity (10^3 J kg^{-1}K^{-1}). Even accounting for various loss mechanisms, it is clear that an object the size of the Earth will be pervasively molten, while an asteroid with a mass 10^6 times smaller will not be heated at all. The Moon-forming impact alone was enough to partially or completely melt the Earth's mantle (Nakajima & Stevenson 2015).

For asteroids, the important heat source is the radioactive element ^{26}Al. This has a half-life of only 0.7 Myr, is therefore currently extinct, and is important only during the first few Myr of solar system history. But during its brief life, ^{26}Al is an effective heat source.

Asteroids that form early enough will inevitably melt due to heating caused by ^{26}Al decay, unless they are small enough (<~30 km radius) that they can conduct the heat away efficiently (e.g. Rubie et al. 2015a). We know that such asteroid melting did occur because of the occurrence of iron meteorites and metallic asteroids, presumably the fragmented cores of once-molten objects. By analogy, most of the objects accreting to the proto-Earth were probably already themselves differentiated into a core and mantle.

2.2 How did the core form?

Initially, solar system bodies consisted of intimate mixtures of silicates, metals and (if far enough from the Sun), ices. Upon heating, some of the volatile material may have been lost. Continued heating (Sec 2.1.1) will have resulted in melting, first of the metal (if Fe-S is present), and then of the silicates.

Melting, at least of the iron, is crucial to the differentiation that results in the formation of metallic cores. Although it is energetically favourable for dense metal to sink to the centre of the planet, the real issue is the timescale over which this happens. Because the viscosities of molten materials are much lower than the viscosity of solids, the efficient physical separation of metal from silicates requires elevated temperatures inside the object in question. For small bodies, these elevated temperatures arise because of ^{26}Al decay (Sec 2.1.1). For larger bodies, the heat is provided by impacts, which also deliver metal. In the case of the Earth, it is likely that most objects striking the Earth were themselves already differentiated. As a result, at least for the Earth "core formation" is something of a misnomer, because it is not a single event. Instead, the Earth's core grew primarily through the addition of large, discrete volumes of metal delivered during giant impacts. Because these giant impacts generally result in pervasive melting (Sec 2.1.1), the majority of iron added to the core had to transit a magma ocean, with important implications for the degree of equilibration between iron and silicates (Sec 2.3).

In principle, core formation could occur by relatively slow percolation of molten iron through a mostly-solid silicate framework. Such permeable flow probably happened in asteroids such as parent bodies of the acapulcoites and lodranites, where metal veins are seen (McCoy et al. 1997). Percolation is more efficient if the characteristic (dihedral) angle joining melt and solid is low (Shi et al. 2013), or if the framework is undergoing deformation (Yoshino et al. 2003, though cf. Cerantola et al. 2015).

In the absence of percolation, macroscopic iron bodies may accumulate near the surface, in which case other modes of downwards transport become accessible (Stevenson 1990). One possibility is diapirism: a large blob of molten iron sinks, deforming the rock around it. The rate at which this happens depends mostly on the viscosity of the surrounding rock, since molten iron is only about ten times more viscous than water. If the mantle is molten, diapirs will descend with a timescale measured in hours. A solid mantle within a few hundred K of its melting temperature will permit diapirs to descend on timescales less than of order 1 Myr. For colder mantles, the cores of small impactors may simply get stranded (Marchi et al. 2018); alternatively, diking may occur, in which the stresses imposed by the iron create a fracture in the brittle rock, which the iron then exploits to propagate downwards (Stevenson 1990). A mantle that is molten towards the surface and solid at depth might result in several of these processes operating sequentially. Figure 1 provides a pictorial summary of the likely processes operating for different impactor sizes.

The above mechanisms – percolation, diapirism and diking – are all relevant to the fate of the cores of relatively small impactors striking a proto-Earth if it is not pervasively molten. However, most of the metal delivered to the Earth probably arrived in the cores of large, Moon- to Mars-sized impactors. For such large impacts, the initial state of the Earth's mantle (molten vs. solid) is irrelevant: the stresses imparted by the impact are sufficiently large that both core and mantle will behave like a fluid over the impact timescale. As a result, the transit timescale for the impactor core to reach Earth's growing core is a few hours. For both large and medium-size impacts, an important question is the extent to which the impactor core becomes emulsified as its passes through the mantle. The reason that this matters is that chemical (diffusive) exchange with the mantle can only happen over lengthscales on the order of 1 cm (Rubie et al. 2003). Thus, the degree of emulsification controls the chemical effects of each impact, and is discussed further in Section 2.3. A dike or a diapir descending through solid mantle material will experience minimal emulsification or chemical exchange; for molten mantles the pictures is less clear-cut.

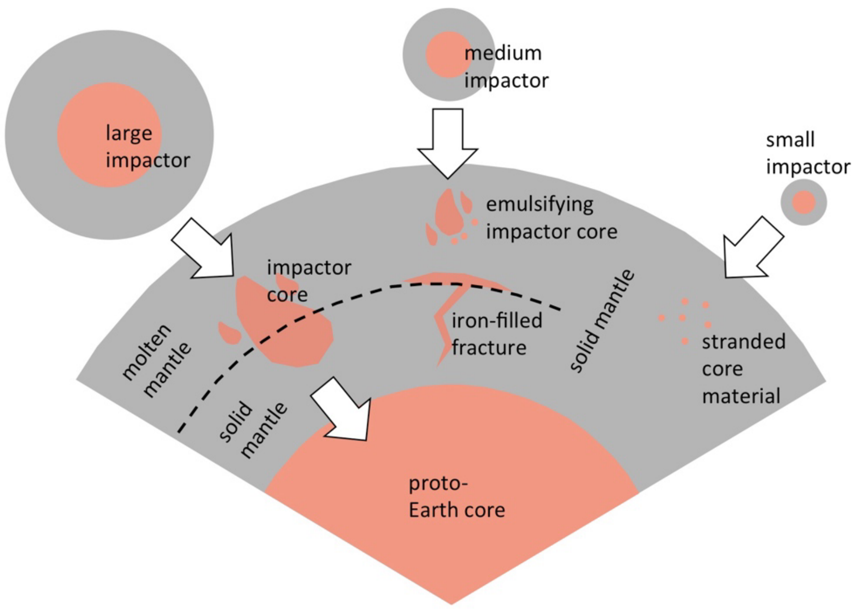

Figure 1. Sketch of possible processes associated with core formation, modified from Nimmo & Kleine (2015). Different size impactors will be associated with different stages or styles of accretion. Figure by the author.

2.3 Timing Constraints

There are several isotopic chronometers which can be used to determine how rapidly the core formed, with the Hf-W (hafnium-tungsten) system being the most useful (Kleine et al. 2009). It is easiest to understand this approach by considering a planet that undergoes a single, instantaneous core formation event. ^{182}Hf decays to ^{182}W with a half-life of 9 Myr.

While the planet is undifferentiated, ^{182}W will accumulate in all regions of the body. However, when differentiation occurs, the tungsten (being siderophile, i.e. metal-loving) will mostly be removed to the core, while hafnium (being lithophile) will be retained in the mantle. If core formation happens early, ^{182}W will continue to accumulate in the mantle as a by-product of the decaying ^{182}Hf. But if core formation occurs too late, the ^{182}Hf will already have decayed completely and no ^{182}W will be produced. Thus, a measure of the concentration of ^{182}W in the mantle, relative to stable isotopes like ^{183}W, can be used to deduce the timing of the formation event. This measure is referred to as the tungsten isotopic anomaly and is defined as ε_{182W}, where

$$\varepsilon_{182W} = \left(\frac{C^{182}_{mantle} / C^{182}_{ref}}{C^{183}_{mantle} / C^{183}_{ref}} - 1 \right) \times 10^4 \qquad (1)$$

where C denotes concentration, superscripts refer to the isotope and the subscript “ref” denotes a reference concentration, often taken to be chondritic. Measurements of the Earth’s mantle Hf/W ratio and tungsten isotopic anomaly give a core formation time of about 30 Myr after CAI (Kleine et al. 2009).

Of course, this apparent “formation time” treats core formation as a single event whereas it is really a consequence of several large impacts, each delivering metal. Nonetheless, the Earth’s tungsten isotope anomaly does allow us to place some constraints on how rapidly the core formed.

In detail, there are two complications. First, the degree to which isotopic re-equilibration happens between each incoming core and the mantle is important. The fraction of the core that equilibrates with the mantle and the fraction of the mantle that equilibrates with the core both matter (Deguen et al. 2014). Higher degrees of re-equilibration reduce the final tungsten isotope anomaly. Thus, because rapid core growth produces a higher tungsten anomaly, there is a tradeoff between the assumed degree of re-equilibration assumed, and the derived age of the core.

Second, the Hf/W ratio of the Earth's mantle almost certainly evolved over time. This is because the degree to which elements partition into metal rather than silicates is not constant. The metal-silicate partition coefficient, *D*, is defined as $D=C_{\mathrm{metal}}/C_{\mathrm{silicate}}$ where *C* denotes concentration and a high *D* implies a siderophile (metal-loving) element. *D* is dependent on pressure, temperature, oxygen fugacity and (in some cases) metal and silicate compositions. Since most if not all of these variables are likely to have changed as the Earth grew, calculations that assume a constant Hf/W are probably too simplistic.

Rather than assuming constant partitioning behavior, recent work has included calculations of how partitioning evolves during accretion. For instance, Rubie et al. (2011) derived the partition coefficients by assuming they were set at P,T conditions in a magma ocean at some fraction of the depth to the core, while the oxygen fugacity (fO_2) was evolved given the initial fO_2 of the precursor materials. Figure 2 shows another such example, from Fischer & Nimmo (2018). Fig 2a shows the growth curves of three Earth analogs, taken from N-body simulations. Fig 2b shows the corresponding evolution of mantle W concentrations; these increase over time because in this model W becomes less siderophile as pressure increases. Finally, Fig 2c shows the evolution of the mantle tungsten anomaly. The initial values are very high, because almost all the W is initially in the core, but the final value in one case (blue line) reproduces the Earth's measured tungsten anomaly.

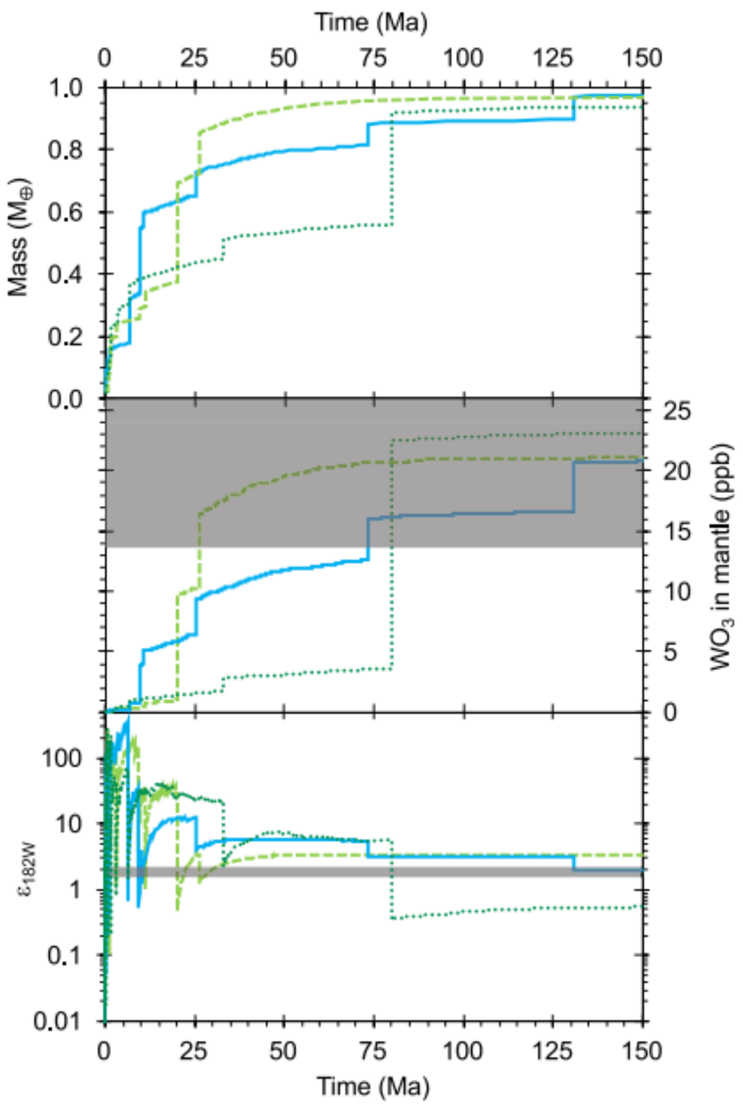

Figure 2. (top panel) Time evolution of Earth-analog mass from 3 N-body simulations. Discontinuities represent giant impacts and major additions of metal to the core. (middle panel) Evolution of mantle tungsten concentration calculated by applying partitioning calculations to the planet growth curves. Shaded region denotes inferred terrestrial value. (bottom panel) Tungsten anomaly (equation 1) as a function of time (note log scale). The initial tungsten anomalies are large because tungsten is very siderophile at low pressures. Reproduced from Fischer & Nimmo (2018).

The issue of re-equilibration is more problematic, because there is as yet little understanding of the fluid dynamics of giant impacts. Simulations of individual impacts using smoothed-particle hydrodynamics (SPH) do not have the resolution to determine what happens at the cm-scale of interest. Laboratory experiments have provided some insight (e.g. Landeau et al. 2021), but the issue remains very much open. Unfortunately, this question matters a lot: one problem with the Grand Tack is that it builds the Earth so fast that it can't reproduce the observed tungsten anomaly – unless re-equilibration is very efficient (Zube et al. 2019). At present it is not clear whether such efficient re-equilibration is plausible, or not.

Although the Hf-W system is the main work-horse, other isotopic systems can also be used, in particular the Pd-Ag and U-Pb systems. While otherwise similar to the Hf-W system, these alternatives both suffer from the fact that one component (Ag and Pb) is volatile. As a result, unlike for refractory Hf and W, we cannot assume that the bulk Earth concentration of these elements is chondritic (e.g. Schoenbachler et al. 2010). This introduces extra uncertainties into the core formation timescales inferred. One solution is to combine the U-Pb and Hf-W systems, allowing simultaneous solution of both the core formation timescale and the degree of equilibration (Rudge et al. 2010). The results give an apparent formation timescale of 80-200 Myr, which is certainly consistent with the N-body results (Fig 2). They also imply that ~40% of the metal re-equilibrated with the silicates, assuming the entire mantle was involved; if a smaller fraction of the mantle was involved, more of the metal would have had to equilibrate (see Deguen et al. 2014).

2.4 Summary

Core formation occurs when internal temperatures become high enough for partial or complete melting to occur. For small bodies, this arises because of heating caused by the decay of ^{26}Al; for larger bodies, the heating arises from the conversion of gravitational energy to heat during impacts. The Earth's core did not form in a single instant, but during a series of collisions with differentiated protoplanets. Assuming a single core formation event, the measured tungsten anomaly gives a core formation timescale of ~30 Myr. Calculations of multi-stage core formation and isotopic evolution using N-body models can reproduce the measured tungsten anomaly. However, there is a tradeoff between how fast the core is required to grow, and how much re-equilibration between iron and silicates is assumed.

3. Composition

3.1 Bulk structure

Because some of the arguments below depend upon it, a brief discussion of the present-day core structure is required. The core consists of a solid inner core of radius 1220 km, surrounded by a convecting liquid outer core that extends out to a radius of 3480 km. The outer core has a seismologically anomalous ("F") layer a few hundred km thick at its base (e.g. Zou et al. 2008); this could be the result of an increase in light element concentrations with increasing radius (Gubbins et al. 2004). There might be a low-density layer immediately beneath the core-mantle boundary (CMB); seismological observations are disputed (Helffrich & Kaneshima 2010, cf. Irving et al. 2018), while length-of-day variations provide some support (Buffett et al. 2016). The solid inner core consists of an anisotropic and hemispherically dichotomous inner region surmounted by an overlying thinner (60-80 km) isotropic region on top (Deuss 2014).

The temperature structure of the core is pinned by that at the inner-core boundary (ICB), which is a liquid-solid phase transition (Hirose et al. 2013). This temperature is probably around 5500 K, although uncertainties in the equation of state and the alloying effect of light elements could change this by perhaps 500 K. Based on projections down the adiabat from the ICB, the temperature at the top of the core, immediately below the CMB is around 4200 K (e.g. Nimmo 2015).

The heat flux out of the core is determined by the temperature structure and dynamics of the mantle. If the anomalous layer at the base of the mantle, termed D'', represents a simple boundary layer then the global heat flow across the CMB is about 13 TeraWattss (TW) (Wu et al. 2011). Seismological observations of the depths of the perovskite-to-post-perovskite phase transition, which provide a temperature estimate, yield a heat flow of around 9 TW when extrapolated globally from the restricted regions in which the phase transition has been detected (Nakagawa & Tackley 2010). A range of 9-15 TW encompasses most of the available estimates (Nimmo 2015).

Based on cosmochemical arguments, the core probably contains about 5.3 wt% Ni (McDonough 2003). More importantly, the bulk density of the core is 7-10% lower than that of an Fe-Ni liquid, implying the presence of one or more light elements, while the seismic velocity is higher than expected (see Sec 3.2). Similarly, the density jump at the ICB of 820+/-180 kgm^{-3} (Masters & Gubbins 2003) is too large to be explained by a phase transition alone, and implies that the outer core is more enriched in light elements than the inner core. Figure 3 summarizes the constraints discussed in this section.

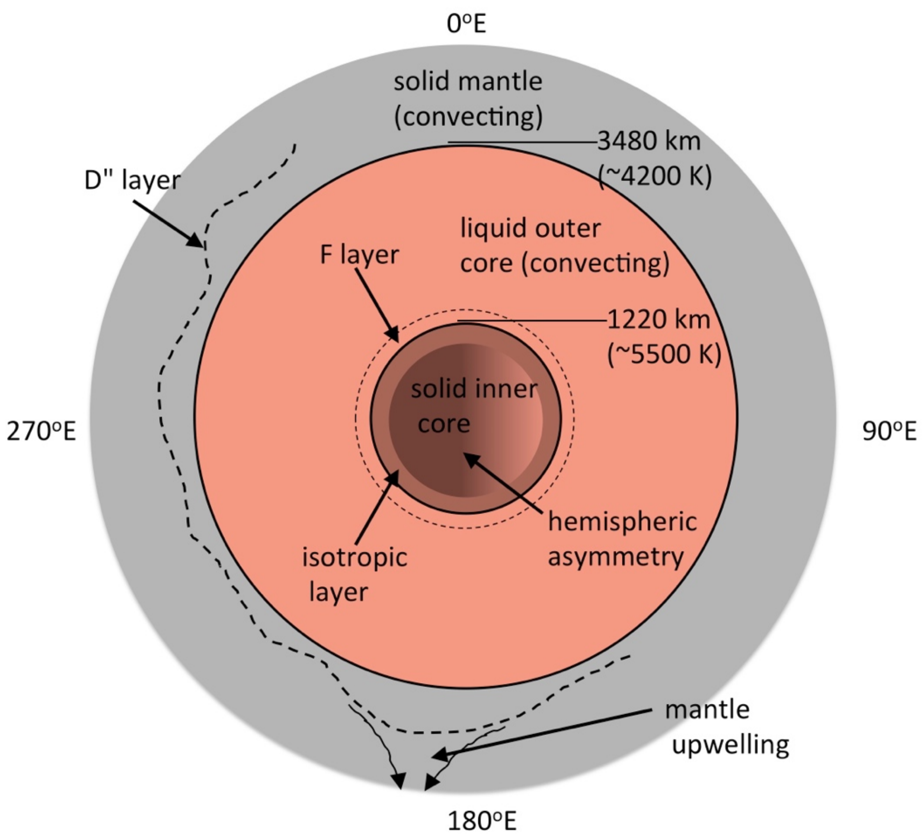

Figure 3. Internal structure of the core, after Litasov & Shatskiy (2016). Note that only the lowermost mantle is shown. The innermost inner core is anisotropic and shows a hemispheric asymmetry. The might be a buoyant layer immediately beneath the CMB, but its existence is disputed (see text). Figure by author.

3.2 Light Elements

As noted above, the core is thought to contain one or more light elements, of which the most likely candidates are O, Si, S, C and H (Poirier 1994). These elements are important for three main reasons. First, they affect the physical properties of the core, notably in reducing the electrical and thermal conductivity (Sec 4.1.1), and reducing the melting temperature. Second, expulsion of some of these elements during inner core solidification is largely responsible for driving the present-day Earth dynamo, while earlier exsolution upon cooling may have contributed to an ancient dynamo (Sec 4.2). And third, if we could identify which elements were present, that would place strong constraints on conditions (such as oxygen fugacity) pertaining during Earth's accretion (Sec 3.2.3).

However, the identity of the light element(s) in the core has been a difficult puzzle to solve for more than 40 years (e.g. Ringwood 1977). In principle, there are two main approaches. The first, direct, approach is to compare the seismically-measured density and sound velocities of Earth's core to experimental measurements on candidate core materials, thus differentiating between the possible components. Unfortunately, this approaches typically produces non-unique answers (e.g. Badro et al. 2014, Umemoto & Hirose 2020) and has also been limited by the difficulty in achieving core pressures and temperatures in experiments. An exception is the inner-outer core density difference, which strongly implicates the presence of oxygen (Sec 3.2.2). The second, modeling, approach is to use accretion and partitioning models to infer the core composition. This approach is less direct;

the results may be very dependent on the starting assumptions, and relies on limited partitioning data from high pressure/temperature experiments. The relative lack of consensus on the nature of the light element(s) is a reflection of the problems inherent in the two approaches described. A combination of the two approaches (e.g. Badro et al. 2015) may help to reduce the uncertainty, but at present it seems unlikely that there will be a definitive answer any time soon.

3.2.1 Density and Elastic Moduli

Measuring the sound velocities of candidate core materials under realistic P,T conditions is hard. Shock experiments have been used (e.g. Zhang et al. 2016), but such experiments typically do not get the correct P and T conditions simultaneously. Static experiments usually use X-ray diffraction in a laser-heated diamond anvil cell to determine the density and X-ray scattering or acoustic measurements to determine sound velocities of the sample. Examples of the latter technique can be found for iron doped with most candidate light elements.

For example, both Edmund et al. (2019) and Nakajima et al. (2020) found that Si as the single light element could not simultaneously explain the observed density deficit and seismic velocity excess. The latter authors suggest that the core may have contained more Si early in its history but that the composition evolved over time (Sec 4.3).

A similar problem arises with carbon. Nakajima et al. (2015) found that 4-5at.% carbon could explain the observed velocities, but was insufficient to account for the density deficit. The conclusion that carbon is not a major constituent is reinforced by partitioning models (Sec 3.2.3). Likewise, Huang et al. (2011) argued on the basis of shockwave data that oxygen alone could not satisfy the observational constraints.

Conversely, Kawaguchi et al. (2017) found that both the density and seismic velocity could be simultaneously explained if the core contained about 6wt.% (10at.%) of sulphur.

However, the inner-outer core density difference is hard to explain with S alone, because S is not excluded during solidification (see Sec 3.2.2); furthermore, experiments show that S does not partition sufficiently strongly into the core at high P-T conditions to produce 6wt% (Suer et al. 2017).

Lastly, hydrogen is particularly challenging from an experimental stand-point. Tagawa et al. (2016) used high-pressure density measurements to argue for up to 0.3 wt% H in the core. However, the seismic velocity was not measured, and the H abundance deduced depended on the assumed concentration (6.5 wt%) of Si present.

Most of the studies cited above focus on a single element, because of the experimental challenges. In reality, however, one might expect several light elements to be present, in which case the single-element conclusions quoted above do not hold. One helpful simplification is that the assumption of perfect mixing works well (Badro et al. 2014, Huang et al. 2019), allowing the behavior of mixtures of different elements to be calculated from the end-member characteristics. Thus, for instance, Morard et al. (2013) used experiments on Fe-S and Fe-Si alloys to deduce core compositions of 6 wt%S and 2wt% Si, or 2.5wt%S and 4-5wt% Si. This result illustrates the commonly-found tradeoff between S and Si.

As an alternative to difficult experiments, some workers have used molecular dynamics or ab initio simulations, in which the physical properties (elastic moduli, densities) of plausible liquids are obtained by directly calculating the interactions between a relatively small number of atoms. Badro et al. (2014) found that all models able to reproduce the measured outer core properties contained some oxygen, in combination with any of S, Si, C (or some mixture of these elements). Umemoto and Hirose (2020) also included H in the mix, and obtained best-fit models favoring a combination of H, O and S. Higher assumed core temperatures require fewer light elements overall, due to the core's thermal expansivity. Li et al. (2018) carried out a similar analysis for the inner core and found that C, combined with

Si and/or S, could reproduce the inner core velocities and density. They did not, however, consider the effect of either H or O.

3.2.2 Inner Core

The inner core provides additional information on the light elements present, for two reasons. First, because it is solid we have two seismic velocities, rather than one, to use as constraints. Second, knowing how elements partition between solid and liquid metal helps us to identify the causes of the measured density and seismic velocity variations. The most important datum is that the inner-outer core density contrast is larger than can be explained by phase changes alone (Sec 3.1). This means that the outer core contains a higher concentration of light elements than the solid inner core.

A particularly influential paper was Alfe et al. (2002), which used ab initio techniques to show that oxygen was excluded much more strongly from the solid than either S or Si. Using an updated core density contrast, Alfe et al. (2007) argued that ~4.3 wt% oxygen had to be present in the outer core, along with 4.6wt% S or Si. The exclusion of oxygen from solid iron was later confirmed by experimental measurements (Ozawa et al. 2010). This is probably the strongest argument for the presence of O in the outer core.

3.2.3 Partitioning Models

An alternative to using density and seismic velocity measurements is to create a model of how the Earth accreted and use it to predict the resulting concentrations of elements in the mantle and core. In general, these studies find that O and Si tend to partition most readily into the core at the P-T conditions relevant to core formation (e.g. Tsuno et al. 2013).

Central to this approach is the acquisition of metal-silicate partitioning data at high pressures and temperatures, using a laser-heated diamond anvil cell or large volume press. Frequently the available data have to be extrapolated to higher pressures and temperatures, and/or different oxygen fugacities and compositions, which can sometimes cause problems

(Siebert et al. 2013). Diamond-anvil cell results are less subject to the extrapolation problem, but interpretation can be complicated because of high temperature gradients across the samples (Kavner & Panero 2004). The difficulty of obtaining reliable partitioning data should not be underestimated: for example, Jennings et al. (2021) document the very different W partitioning behavior obtained by different groups.

Modeling Earth's core formation requires various poorly-known parameter values to be chosen. Of these, the most important are the initial oxidation state of the starting material; the P,T conditions at which metal and silicates equilibrated; the fraction of metal that equilibrates with the silicates (Sec 2.3), and the fraction of silicates that equilibrates with the metal . Once these parameters are fixed, the partitioning of elements between metal and silicates can be tracked as the model Earth grows (Figure 2), and the final concentrations calculated. The parameters can be varied to obtain the best fit between the calculated mantle values and the actual concentrations (as inferred from peridotite nodules).

A good example of this kind of study is Rubie et al. (2015b), which concluded that the core contains 2-4 wt%O, 8-9wt% Si and 9-58ppm H (C and S were not modeled). Apart from sensitivity to the initial compositions assumed, an important caveat is the large extrapolations in experimentally-determined partition coefficients. Fischer et al. (2020) used higher-pressure partitioning data and found that carbon becomes increasingly less siderophile as P,T increase. As a result, their models suggest a maximum of 0.2 wt% C in the core, although this conclusion may be sensitive to the particular oxygen fugacity history assumed. In Badro et al. (2015)'s hybrid approach, constraints on the core velocity and density were used in addition to mantle element concentrations to identify successful accretion scenarios. Unlike Rubie et al., this approach assumes a trajectory for oxygen fugacity, rather than calculating it in a self-consistent fashion (although the Rubie et al. approach still requires assumptions to be made regarding starting compositions).

3.2.4 Hydrogen and noble gases in the core

Attempts to constrain core hydrogen abundances from partitioning include those of Malavergne et al. (2019) and Yuan & Steinle-Neumann (2020). The first used experiments to infer an upper limit of 0.3 wt%H; such experiments are technically very challenging because of the tendency of H atoms to diffuse rapidly out of liquid iron during the quench phase of the experiment. The latter used ab initio calculations to obtain an upper bound of 1wt%. Neither of these papers, however, did the kind of multi-stage partitioning calculations discussed above.

Any such hydrogen partitioning model suffers from the large uncertainty in the pre-partitioning (bulk Earth) H abundance. This is for three main reasons. First, H_2O is volatile and so chondritic compositions do not provide a useful guide as to how much H was initially present. Second, the present-day H concentration in the Earth's mantle is very uncertain because of an absence of representative samples and the difficulty in constraining the H fluxes into and out of the mantle (Hirschmann 2006). Third, we have no idea whether the Earth's H budget was added during the main phase of accretion (in which case some could have been sequestered into the core), or was added subsequently as a "late veneer".

Early addition of H (either as ice or as gas) has problems not associated with the other, more refractory, elements. The problem is that the nebular dissipation (H loss) timescale is ~3 Myr (e.g. Wang et al. 2017), while core formation took more than 30 Myr to complete (Sec 2.3). The proto-planets that eventually made up the Earth may have been initially enveloped in a cloud of primordial nebular gas (Ikoma & Genda 2006). But since these bodies were probably differentiated, acquisition of H to their cores would have required passage of H into the supervening magma ocean, followed by diffusive exchange. Alternatively, equilibration during impacts could have transferred H from silicates to metal – but impacts are a good way of removing H, and are likely responsible for the apparent loss of other volatiles like carbon (Hirschmann et al. 2021). Similarly, delivery of H-rich impactor cores to the proto-Earth suffers from the difficulty of likely H loss during the extremely energetic impact itself. At least to this author it seems likely that the Earth's core did not acquire significant amounts of H during its prolonged accretion.

A similar set of arguments applies to noble gases such as He and Ne, which are certainly of nebular origin and are stored in small quantities within the Earth (Honda et al. 1993). Partitioning experiments show that, in principle, they could be sequestered into the core if in contact with nebular gas (Bouhifd et al. 2020). However, these gases could equally well have been acquired by dissolving into an early magma ocean (Olson & Sharp 2019).

3.2.5 Mg/Si and Si Isotopes

It has been argued that two observations point to Si in the core (Fitoussi et al. 2009). One is that the Earth's (mantle) Mg/Si ratio is somewhat larger than that of primitive chondritic material. The other is that the Earth's mantle has an Si isotopic composition that is heavier than that of chondrites. These observations could be explained simultaneously by sequestering Si into the core.

However, further work argues against this hypothesis. In particular, the angrite parent body, which formed a core under very different circumstances to the Earth, also demonstrates a heavy Si isotopic signature (Dauphas et al. 2015). This argues strongly against the Earth's heavy Si being due to core formation, and alternative mechanisms (such as evaporative loss in precursor materials) are available. Of course, even if this argument does not hold, that does not rule out Si as a possible core contaminant, and indeed it seems likely that Si is present (Sec 3.2.1).

3.2.6 Radiogenic elements

The incorporation of even small concentrations of radiogenic elements (K,U,Th) into the core would have significant effects on core behavior and evolution. Although the extra impetus provided to the dynamo is minor, the extra heat production can substantially slow core cooling and delay the onset of inner core formation (Nimmo 2015). Although K in particular has been presented as a possible core contaminant, recent ab initio (Xiong et al. 2018) and experimental (Blanchard et al. 2017) partitioning approaches both derived a core K concentration of about 30 ppm, too small to have any important effect on core evolution.

3.2.7 Summary

Despite great progress in high-pressure experimental techniques, the identity of the light element(s) in the core remains elusive, primarily because of the paucity of observational constraints. Nonetheless, some conclusions can be drawn. Based on the density contrast at the ICB and the majority of partitioning and velocity/density studies, a few percent O seems almost inescapable. Conversely, partitioning data and volatile-loss arguments (Hirschmann et al. 2021) do not favour the presence of significant amounts of C, while water-delivery arguments argue against much H being present. Since the velocity/density data are hard to fit with a single element, S or Si (or both) are likely present in addition to O, with Si probably more abundant. Figure 4 provides a graphical summary of selected partitioning and experimental studies. Almost all studies include some O; this figure also shows the tradeoff between S and Si noted above, and that the preponderance of studies favour Si over S.

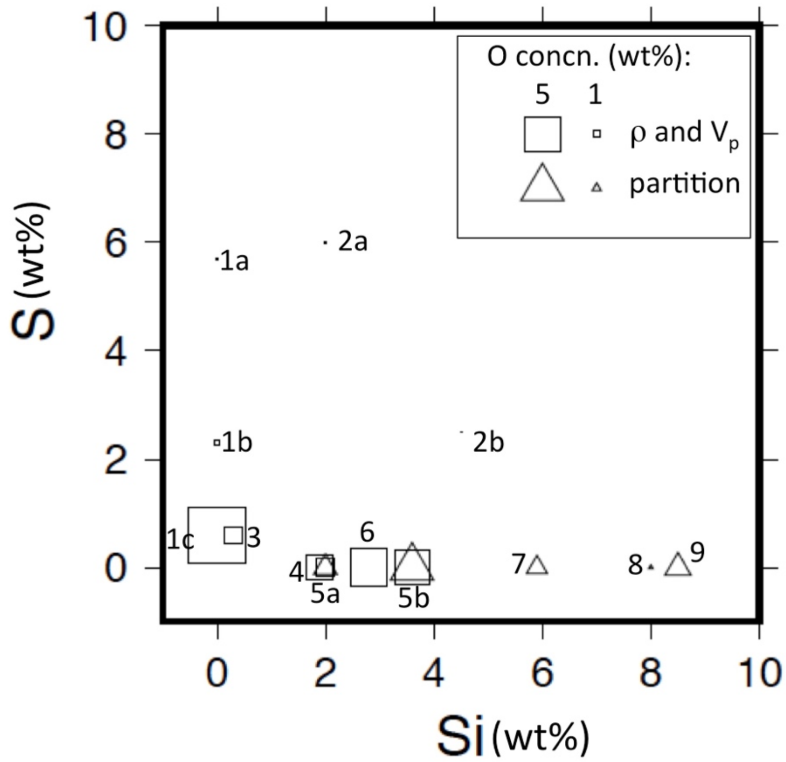

Figure 4. Estimated core compositions from selected studies. Symbol size is proportional to wt% of O present; symbol type indicates nature of constraint (partitioning or material properties). Numbers indicate publication: 1-Huang et al. 2011; 2-Morard et al. 2013; 3-Umemoto & Hirose 2020 (all at 5400 K); 4-Badro et al. 2014; 5-Badro et al. 2015; 6-Badro et al. 2007; 7-Fischer et al. 2015; 8-Rubie et al. 2011; 9-Rubie et al. 2015b. Figure by author.

4. Evolution

The most important parameter controlling the evolution of the core is its cooling rate. This is because the growth of the inner core, the maintenance of the dynamo, and the potential exsolution of light elements all depend on the core temperature. This cooling rate is in turn controlled by the behavior of the mantle above, as it is the mantle's ability to extract heat that is the rate-limiting process. Thus, core evolution cannot be separated from the long term thermal evolution of the Earth's mantle (Nakagawa 2020).

4.1 Thermal evolution

Reconstructing the thermal evolution of the core is not quite as intractable as it might at first appear, because any successful model has to satisfy the magnetic constraints. As discussed in Sec 4.2, the Earth's dynamo has operated continually since at least 3.5 Gyr B.P. Because the dynamo is ultimately powered by heat being extracted from the core, the dynamo's existence thus places a lower bound on the rate of heat extraction over time. In the absence of an inner core, the minimum heat flow required to keep the dynamo operating is the so-called adiabatic value, given by

$$4\pi R_c^2 F = 4\pi R_c^2\, k\, \alpha\, g_c\, T / C_p = 11.5 \text{ TW } (k / 100 \text{ Wm}^{-1}\text{K}^{-1}) \qquad (2)$$

where F is the heat flux, α is the thermal expansivity, g_c the acceleration due to gravity at the CMB evaluated using the central core density (12.2 ms^{-2}), T the temperature, C_p the specific heat capacity, R_c the core radius and k the thermal conductivity. All but the last of these are reasonably well-known (specific values are taken from Nimmo 2015), but the thermal conductivity is uncertain, by a factor of perhaps 3 (Sec 4.1.1). This translates into a correspondingly large uncertainty in the minimum heat flux and thus the core's evolution.

4.1.1 Thermal conductivity

Starting around 2012, estimates of core conductivity were revised sharply upwards, significantly changing core evolution scenarios. Ab initio calculations of conductivity produced values of 90-150 Wm^{-1}K^{-1} (de Koker et al. 2012, Pozzo et al. 2012), much higher than the earlier consensus value of ~40 Wm^{-1}K^{-1} (e.g. Stacey & Anderson 2001). Static Fe electrical conductivity experiments, when converted to thermal conductivity, gave similar results (Gomi et al. 2013). Unfortunately, further experiments have muddied the issue, with Fe electrical conductivity measurements (Ohta et al. 2016) yielding dramatically higher values than a direct measurement of Fe thermal conductivity (Konopkova et al. 2016): 200-300 $Wm^{-1}K^{-1}$ and 18-44 $Wm^{-1}K^{-1}$, respectively. A recent DAC electrical conductivity experiment by Zhang et al. (2020) gave a value of 100 $Wm^{-1}K^{-1}$. First principles calculations by Xu et al. (2018) suggest a value of 77±10 $Wm^{-1}K^{-1}$. Hsieh et al. (2020) made direct experimental thermal conductivity measurements and derived an iron thermal conductivity value of about 60 $Wm^{-1}K^{-1}$, but with a reduction to 20 $Wm^{-1}K^{-1}$ in the presence of 15wt% Si.

This last result illustrates an important additional complication: the real core, unlike most of the experimentally-studied samples, contains impurities (Si, O etc. – see Sec 3.2). These typically reduce thermal conductivity by ~2-4% per wt% of impurity added (Williams 2018). But since the identity and concentrations of the impurities are uncertain, the total reduction in conductivity is also uncertain.

In short, as reviewed by Williams (2018), there is no consensus on the best value of thermal conductivity to adopt. More studies favour higher (~100 $Wm^{-1}K^{-1}$) values, but the majority is not always right.

4.1.2 Thermal Evolution

The dominant factor controlling the thermal evolution of the core is the rate at which the mantle is extracting heat, that is the core-mantle boundary (CMB) heat flux (Sec 3.1). Given this, two basic approaches to modeling long-term core thermal evolution are employed. One is to simply specify the CMB heat flux, either directly or via constraints imposed by the existence of the dynamo; this has the advantage of removing any need to explicitly model the mantle's behavior. The other is to model the whole Earth system, and hence calculate the CMB heat flux directly. This approach requires many more poorly-known parameters, such as a description of how the Earth's surface heat flux has evolved over time.

The first approach is perhaps less realistic, but is certainly simpler. Both Labrosse (2015) and Nimmo (2015) adopted this approach and obtained very similar answers, summarized here. Prior to inner core formation, a dynamo will operate if the CMB heat flux exceeds the minimum (adiabatic) required value (equation 2). The biggest uncertainty in this minimum heat flux is the core thermal conductivity (Sec 4.2.1). A CMB heat flux of around 9-15 TW has some support from mantle observations (Sec 3.1), and would be marginally sufficient to allow a pre-inner-core dynamo to operate with k= 80-130 $Wm^{-1}K^{-1}$. With a heat flow of 15 TW, the inner core is only 0.5-0.6 Gyr old. A lower thermal conductivity of 40 $Wm^{-1}K^{-1}$ would allow a lower minimum present-day CMB heat flow (~5 TW) and therefore permit a more ancient inner core with an age of ~1.5-2 Gyr B.P.

When an inner core is present, the minimum CMB heat flux required to keep a dynamo operating is reduced below the level given by equation (2). This is because light elements expelled from the solidifying inner core provide a buoyancy source that is additional to the always-present thermal buoyancy. Thus, even a subadiabatic CMB heat flux can maintain a dynamo if a growing inner core is present; this may have the interesting consequence of producing stably stratified regions near the top of the core (Labrosse 2015, Nimmo 2015), though the existence for such regions is weak (Sec 3.1).

As long as the CMB heat flow exceeds the critical value there is no problem in maintaining the geodynamo for all of Earth history; the inner core is *not* required for the dynamo to exist. Conversely, the apparent existence of the geodynamo for at least the last 3.5 Gyr places constraints on the evolution of the CMB heat flow.

In the second approach, the CMB heat flow is calculated based on the thermal evolution of the mantle. This can be accomplished in one of two ways. One is to do a direct numerical simulation of mantle convection and plate tectonics. This is computationally expensive, even in 2D (e.g. Langemeyer et al. 2018). The alternative is to use a parameterized description of convection, essentially a 1D approximation of heat transfer focusing on the boundary layers (e.g. Davies 2007). This is faster, but may miss important physics that the more complex numerical models can include. In both cases, many poorly-known parameters have to be specified and the models become increasingly less constrained and less reliable as they go back further in time.

An example of the first class of model is Nakagawa and Tackley (2015), in which a sophisticated 2D thermo-chemical model is used to explore how varying the frictional resistance of rock controls the tectonic style of the planet and thus the survival or demise of the dynamo. An example of the second approach is Nimmo et al. (2020), from which Figure 5 is adapted. Panels (a) and (b) show the evolution of temperatures and heat flows of interest; the core cools sufficiently to initiate inner core formation at about 1 Gyr B.P. Panel (a) also shows the rate of excess entropy production, a proxy for dynamo strength. This drops almost to the critical value of zero at which dynamo failure would occur, before being rescued by the onset of inner core growth, which provides additional buoyancy flux. Here the value of *k* adopted is 50 $Wm^{-1}K^{-1}$, resulting in an intermediate-age inner core.

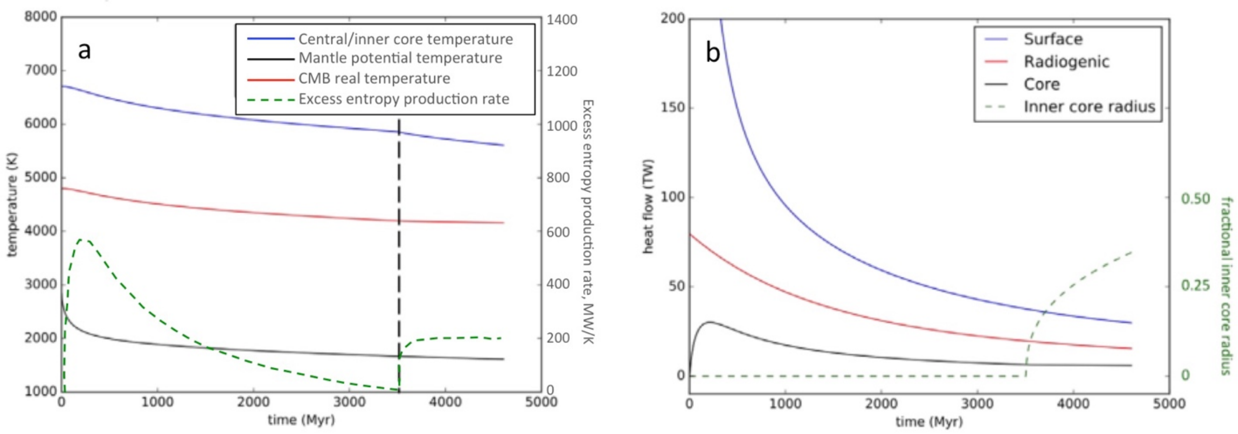

Figure 5. a) Parameterized thermal convection model showing evolution of central core, mantle potential[1] and CMB actual temperatures. The green dashed line (right-hand scale) shows the excess entropy production rate, a proxy for dynamo strength. The vertical dashed line shows when the inner core forms. b) Evolution of core, mantle and radiogenic

[1]For an adiabatic (convecting) mantle, the potential temperature is the temperature extrapolated along the adiabat to the surface.

heat flows, all evaluated at the surface. Green dashed line shows the growth of the inner core. Modified from Nimmo et al. (2020).

4.1.3 Growth and Age of the Inner Core

As noted in Sec. 4.1.2, the inner core age depends primarily on the CMB heat flow; basically, the inner core age equals the current inner core radius divided by its growth rate, which scales with the heat flow. Likely CMB heat fluxes imply an inner core age in the range 0.5-2 Gyr B.P. Paleomagnetic data have been used to argue both for the younger end of this age range (Bono et al. 2019) and the older end (Biggin et al. 2015).

The structure of the inner core (Fig 3) presumably provides a record of its growth. One possibility is that it arises from translational motion of the core being balanced by freezing/melting (e.g. Alboussiere et al. 2010); alternatively, convection of the solid inner core might lead to anisotropic crystal alignments (e.g. Cottaar & Buffett 2012). Unfortunately, neither class of models casts additional light on the age of the inner core.

4.2 Magnetic evolution

As discussed in Sec 4.1.2, the magnetic evolution of the core is directly tied to its thermal evolution. Heat extracted from the core can drive core thermal convection or (if cooling produces inner core growth) compositional convection; either kind of convection can in turn drive a dynamo. Thus, the history of the Earth's magnetic field tells us about the thermal evolution of the core.

The Earth's magnetic field has certainly operated for the last 3.5 Gyr, and there is some evidence, though it is controversial, of fields as old as 4.2 Ga (Tarduno et al. 2020). In general, the estimated strength of the magnetic field does not appear to have changed systematically with time. In particular, there is no obvious uptick in the field strength at the estimated time of inner core formation, which would be expected from modeling. The explanation is most likely that the scatter in the data is larger than the estimated uptick size

(Labrosse 2015). However, it has been argued (Bono et al. 2019) that the field at 0.565 Gyr B.P. - immediately before the likely IC formation age – is anomalously low. Perhaps this is an indication that the dynamo nearly shut down, before being providentially rescued by inner core formation. Conversely, it has also been argued that the field increased in strength and variability in the period 1-1.5 Gyr B.P., suggesting an older inner core onset (Biggin et al. 2015).

Dynamo simulations show that the CMB heat flow and the inner core size can both affect details of the magnetic field like its temporal stability, axial alignment and dipolar vs. multipolar behavior, as well as its strength (e.g. Driscoll 2016). The spatial distribution of heat extraction on the mantle side of the CMB can also affect the field characteristics (Olson 2016). Unfortunately, pre-Cambrian paleomagnetic measurements are sparse and mostly just yield field intensities and not these other field characteristics.

4.3 Chemical evolution

The chemical evolution of the core can be divided into three main topics: inner core solidification; exsolution; and core-mantle interactions.

Inner core solidification is the most straightforward. As the metal solidifies, it expels light elements like oxygen (Sec 3.2). The light fluid released rises, driving core circulation as it does so. This compositional buoyancy is a major driver of the present-day geodynamo. The well-mixed outer core thus becomes progressively enriched in light elements, although the small volume of the inner core (4% of the total) means that the composition of the present-day outer core is not very different from the initial, bulk core composition.

Solubility of elements in metals typically decreases with decreasing temperature. Thus, if part of the core last equilibrated with mantle materials at high temperatures – likely because of the giant impacts involved in core formation (Sec 2.1.1) - Mg and Si initially dissolved in the metal may at some point have exsolved as the core cooled (Badro et al. 2016, Hirose et al. 2017). This exsolution process is potentially important because it provides another source of compositional buoyancy to drive the dynamo, and the exsolution products will tend to form a stably-stratified layer at the top of the core. Observational evidence for any such layer is controversial (Sec 3.1).

A closely related driver of core chemical evolution is interactions with the mantle. Diffusive exchange with the solid mantle is prohibitively slow, but if the base of the mantle was molten (e.g. Labrosse et al. 2007), more exchange would have happened. The chemistry is not fundamentally different to the exsolution scenario described above, although the dynamics and timescales involved are quite different. Thus, for instance, Si and O will dissolve into the core from lower-mantle minerals (e.g. Bouhifd & Jephcoat 2011). Buffett and Seagle (2010) describe the dynamics of the resulting growing, buoyant layer and find a present-day thickness of tens of km. A layer this thin is unlikely to have large long-term effects on the thermal evolution of the core; a stably stratified sub-adiabatic layer (Sec 4.1.2) could be thicker and have much more significant effects, but few studies have addressed this issue (Lister and Buffett 1998).

4.4 Summary

The core has cooled fast enough for at least the past 3.5 Gyr to maintain a dynamo. Prior to the formation of the inner core, the CMB heat flow had to exceed the adiabatic value (equation 2), which could be as low as 5 TW or as high as 15 TW. The uncertainty arises from the current large uncertainty in the core thermal conductivity. The inner core could have formed as recently as 0.5 Gyr B.P., or as long ago as 1.5-2 Gyr B.P.; paleomagnetic measurements have been used to support both ages. The high temperature of core formation may have initially dissolved Mg and Si, which subsequently exsolved as the core cooled. Additional minor addition of Si and O to the core may have arisen via interactions with silicate melt in the lowermost mantle.

5. Conclusions

The findings discussed in this chapter may be summarized as follows. Earth's core formed mainly by the delivery of metal during giant impacts over an extended (tens of Myr) period. The core contains light elements acquired during the accretion process: almost certainly oxygen, very likely silicon, and perhaps sulphur as well. The long term thermal evolution of the core is controlled by the mantle's ability to extract heat. So too is the existence of a dynamo, but the actual CMB heat flow required for a dynamo is currently uncertain because of the large uncertainties (more than a factor of 3!) in the thermal conductivity of the core. As the core cooled, the inner core grew, but its age is also uncertain (0.5-2 Gyr B.P.). Si and possibly Mg originally dissolved in the hot early core may have exsolved as it cooled, thus forming a buoyant layer at the CMB.

There are several obvious future avenues of research to pursue. Perhaps the most important is a resolution of the thermal conductivity issue (Sec 4.1.1), by direct experimental measurements. A second is the issue of how much core-mantle equilibration occurs (Sec 2.3), which probably also requires laboratory techniques. Partitioning studies (Sec 3.2.3), especially when combined with unstable isotopes (Sec 2.3), provide a powerful way of probing how and when the core accreted; further high-pressure partitioning experiments are desirable, and so too are models probing the different proposed pathways for Earth formation, such as pebble accretion (Sec 2.1).

Conversely, the issue of the core light element content seems unlikely to be resolved any time soon, simply because of the degeneracies in the available constraints. Likewise, the early history of the core and dynamo are unlikely to be solved, because there are too many free parameters in the models and not enough paleomagnetic or geodynamic constraints. Nonetheless, perhaps the most important lesson of this review is that the core cannot be treated in isolation: its evolution is tightly coupled to the behavior of the overlying mantle. Ultimately, a full understanding of the core requires a whole Earth perspective.

Acknowledgements: The author thanks James Badro, Rebecca Fischer and especially Dave Rubie for detailed and helpful comments.

References

Alboussiere, T., Deguen, R., & Melzani, M. (2010) Melting-induced stratification above Earth's inner core due to convective translation. *Nature 466*, 744-746.

Alfe, D., Gillan, M.J. & Price, G.D. (2002) Composition and temperature of the Earth's core constrained by combining ab initio calculations and seismic data. *Earth Planet. Sci. Lett. 195*, 91-98.

Alfe, D., Gillan, M.J. & Price, G.D. (2007) Temperature and composition of the Earth's core. *Contemp. Phys. 48*, 63-80.

Asphaug, E. (2010) Similar-sized collisions and the diversity of planets, *Chemie der Erde-Geochemistry, 70,* 199-219.

Badro, J., Cote, A.S. & Brodholt, J.P. (2014) A seismologically consistent compositional model of Earth's core. *Proc. Nat. Acad. Sci. USA 111*, 7542-7545.

Badro, J., Brodholt, J.P., Piet, H., Siebert, J., & Ryerson, F.J. (2015) Core formation and core composition from coupled geochemical and geophysical constraints, *Proc. Nat. Acad. Sci. USA 112*, 12310-12314.

Badro, J., Siebert, J. & Nimmo, F. (2016) An early geodynamo driven by exsolution of mantle components from Earth's core. *Nature 536*, 326-328.

Biggin, A.J., Piispa, E.J., Pesonen, L.J., Holme, R., Paterson, G.A., Veikkolainen, T., & Tauxe, L. (2015) Paleomagnetic field intensity variations suggest Mesoproterozoic inner-core nucleation. *Nature 526*, 245-247.

Bitsch, B., Lambrechts, M. & Johansen, A. (2015). The growth of planets by pebble accretion in evolving protoplanetary disks. *Astron. Astrophys. 582*, A112.

Blanchard, I., Siebert, J., Borensztajn, S. & Badro, J. (2017) The solubility of heat-producing elements in Earth's core. *Geochem. Perspective Lett*. 5, 1-5.

Bono, R.K., Tarduno, J.A., Nimmo, F. & Cottrell, R.D. (2019) Young inner core inferred from Ediacaran ultra-low geomagnetic field intensity. *Nature Geosci. 12*, 143-146.

Bouhifd, M.A. & Jephcoat, A.P. (2011) Convergence of Ni and Co metal-silicate partition coefficients in the deep magma ocean and coupled silicon-oxygen solubility in iron melts at high pressures. *Earth Planet. Sci. Lett. 307*, 341-348.

Bouhifd, M.A., Jephcoat, A.P., Porcelli, D., Kelley, S.P. & Marty, B. (2020). Potential of Earth's core as a reservoir for noble gases: Case for helium and neon. *Geochem. Perspective Lett. 15*, 15-18.

Buffett, B.A., Seagle, C.T. (2010) Stratification of the top of the core due to chemical interactions with the mantle. *J. Geophys. Res. 115*, B04407.

Buffett, B., Knezek, N. & Holme, R. (2016) Evidence for MAC waves at the top of Earth's core and implications for variations in length of day. *Geophys. J. Int. 204*, 1789-1800.

Cerantola, V., Walte, N.P., Rubie, D.C. (2015) Deformation of a crystalline olivine aggregate containing two immiscible liquids: Implications for early core-mantle differentiation, *Earth Planet. Sci. Lett.* 417, 67-77.

Cottaar, S. & Buffett, B. (2012) Convection in the Earth's inner core. *Phys. Earth Planet. Inter. 198*, 67-78.

Dauphas, N., Poitrasson, F., Burkhardt, C., Kobayashi, H. & Kurosawa, K. (2015). Planetary and meteoritic Mg/Si and delta-Si-30 variations inherited from solar nebula chemistry. *Earth Planet. Sci. Lett. 427*, 236-248.

Davies, G.F. (2007) Mantle regulation of core cooling: A geodynamo without core radioactivity? *Phys. Earth Planet. Inter. 160*, 215-229.

Deguen, R., Landeau, M. & Olson, P. (2014) Turbulent metal-silicate mixing, fragmentation and equilibration in magma oceans. *Earth Planet. Sci. Lett. 391*, 274-287.

De Koker, N., Steinle-Neumann, G., & Vlcek, V. (2012) Electrical resistivity and thermal conductivity of liquid Fe alloys at high P and T, and heat flux in Earth's core, *Proc. Nat. Acad. Sci. USA 111*, 4070-4073.

Deuss, A. (2014) Heterogeneity and anisotropy of Earth's inner core. *Ann. Rev. Earth Planet. Sci. 42*, 103-126.

Driscoll, P. (2016) Simulating 2 Ga of geodynamo history, *Geophys. Res. Lett. 43,* 5680-5687.

Edmund, E., Antonangeli, D., Decremps, F. et al. (2019) Velocity-density systematics of Fe-5wt%Si: Constraints on Si content in the Earth's inner core, *J. Geophys. Res. 124,* 3436-3447.

Fischer, R.A. & Nimmo, F. (2018) Effects of core formation on the Hf-W isotopic composition of the Earth and dating of the Moon-forming impact, *Earth Planet. Sci. Lett. 499*, 257-265.

Fischer, R.A., Cottrell, E., Hauri, E., Lee, K.K.M. & Le Voyer, M. (2020) The carbon content of the Earth and its core, *Proc. Nat. Acad. Sci. USA 117,* 8743-8749.

Fitoussi, C., Bourdon, B., Kleine, T., Oberli, F. & Reynolds, B.C. (2009) Si isotope systematics of meteorites and terrestrial peridotites: implications for Mg/Si fractionation in the solar nebula and for Si in the Earth's core, *Earth Planet. Sci. Lett. 287*, 77-85.

Gomi, H., Ohta, K., Hirose, K., Labrosse, S., Caracas, R., Verstraete, M.J. & Hernlund, J.W. (2013) The high conductivity of iron and thermal evolution of the Earth's core, *Phys. Earth Planet. Inter. 224*, 88-103.

Helffrich, G. & Kaneshima, S. (2010). Outer core compositional stratification from observed core wave speed profiles, *Nature 468*, 807-809.

Hirose, K., Labrosse, S. & Hernlund, J. (2013) Composition and state of the core, *Ann. Rev. Earth Planet. Sci. 41*, 657.

Hirose, K., Morard, G., Sinmyo, R., Umemoto, K., Hernlund, J., Helffrich, G. & Labrosse, S. (2017) Crystallization of silicon dioxide and compositional evolution of the Earth's core, *Nature 543*, 99-101.

Hirschmann, M. (2006) Water, melting and the deep Earth H2O cycle, *Ann. Rev. Earth Planet. Sci. 34,* 629-653.

Hirschmann, M.M., Bergin, E.A., Blake, G.A., Ciesla, F.J., Li, J. (2021) Early volatile depletion on planetesimals inferred from C-S systematics of iron meteorite parent bodies, *Proc. Nat. Acad. Sci.* 118, e2026779118.

Honda, M., Patterson, D.B., McDougall, I. & Falloon, T. (1993) Noble gases in submarine pillow basalt glasses from the Lau basin – detection of a solar component in backarc basin basalts, *Earth Planet. Sci. Lett. 120*, 135-148.

Hsieh, W.P., Goncharov, A.F., Labrosse, S., Holtgrewe, N., Lobanov, S.S., Chuvashova, I., Deschamps, F. & Lin, J.F. (2020) Low thermal conductivity of iron-silicon alloys at Earth's core conditions with implications for the geodynamo, *Nature Communications 11*, doi: 10.1038/s41467-020-17106-7

Huang, H., Fei, Y.W., Cai, L.C., Jing, F.Q., Hu, X.J., Xie, H.S., Zhang, L.M. & Gong, Z.Z. (2011). Evidence for an oxygen-depleted liquid outer core of the Earth, *Nature 479,* 513-516.

Huang, D.Y., Badro, J., Brodholt, J. & Li, Y.G. (2019) Ab initio molecular dynamics investigation of molten Fi-Si-O in Earth's core, *Geophys. Res. Lett.* 46, 6397-6405.

Ikoma, M. & Genda, H. (2006) Constraints on the mass of a habitable planet with water of nebular origin, *Astrophys. J. 658*, 696-706.

Irving, J.C.E., Cottaar, S. & Lekic, V. (2018) Seismically determined elastic parameters for Earth's outer core, *Sci. Advances 4*, eaar2538.

Jennings, E.S., Jacobson, S.A., Rubie, D.C., Nakajima, Y., Vogel, A.K., Rose-Weston, L.A. & Frost, D.J. (2021) Metal-silicate partitioning of W and Mo and the role of carbon in controlling their abundances in the bulk silicate Earth, *Geochim. Cosmochim. Acta* 293, 40-69.

Kavner, A., Panero, W.R. (2004) Temperature gradients and evaluation of thermoelastic properties in the synchrotron-based laser-heated diamond anvil cell, *Phys. Earth Planet. Inter.* 143, 527-539.

Kawaguchi, S.I., Nakajima, Y., Hirose, K. et al. (2017) Sound velocity of liquid Fe-Ni-S at high pressure*, J. Geophys. Res. 122*, 3624-3634.

Kleine, T., Touboul, M., Bourdon, B., Nimmo, F., Mezger, K., Palme, H., Yin, Q.-Z., Jacobsen, S.B., Halliday, A.N. (2009) Hf-W chronometry and the accretion and early evolution of asteroids and terrestrial planets, *Geochim. Cosmochim. Acta 73*, 5150-5188.

Konopkova, Z., McWilliams, R.S., Gomez-Perez, N. & Goncharov, A.F. (2016) Direct measurement of thermal conductivity in solid iron at planetary core conditions, *Nature 534*, 99-101.

Labrosse, S., Hernlund, J.W. & Coltice, N. (2007) A crystallizing dense magma ocean at the base of the Earth's mantle, *Nature 450*, 866-869.

Labrosse, Thermal evolution of the core with a high thermal conductivity (2015), *Phys. Earth Planet. Inter. 247*, 36-55.

Landeau, M., Deguen, R., Phillips D., Neufeld, J.A., Lherm, V. & Dalziel, S.B. (2021) Metal-silicate mixing by large Earth-forming impacts, *Earth Planet. Sci. Lett.* 564, 116888.

Langemeyer, S.M., Lowman, J.P. & Tackley, P.J. (2018) The sensitivity of core heat flux to the modeling of plate-like surface motions, *Geochem. Geophys. Geosystems 19*, 1282-1308.

Li, Y.G., Vocadlo, L., & Brodholt, J.P. (2018) The elastic properties of hcp-Fe alloys under the conditions of the Earth's inner core. *Earth Planet. Sci. Lett. 493*, 118-127.

Lister, J.R. & Buffett, B.A. (1998) Stratification of the outer core at the core-mantle boundary, *Phys. Earth Planet. Inter. 105*, 5-19.

Litasov, K.D. & Shatskiy, A.F. (2016) Composition of the Earth's core: A review, *Russian Geol. Geophys. 57*, 22-46.

Malavergne, V., Bureau, H., Raepsaet, C. et al. (2019) Experimental constraints on the fate of H and C during planetary core-mantle differentiation: Implications for the Earth, *Icarus 321,* 473-485.

Marchi, S., Canup, R.M. & Walker, R.J. (2018) Heterogeneous delivery of silicate and metal to the Earth by large planetesimals, *Nature Geosci. 11*, 77-80.

Masters, G. & Gubbins, D. (2003) On the resolution of density within the Earth, *Phys. Earth Planet. Inter. 140*, 159-167.

McCoy, T.J., Keil, J., Muenow, D.W. & Wilson, L. (1997) Partial melting and melt migration in the acapulcoite-lodranite parent body, *Geochim. Cosmochim. Acta 61,* 639-650.

McDonough, W.F. (2003) Compositional model for the Earth's core, *Treatise Geochem. Vol. 2*, p.547-568

Morard, G., Siebert, J., Andrault, D., Guignot, N., Garbarino, G., Guyot, F. & Antonangeli, D. (2013) The Earth's core composition from high pressure density measurements of liquid iron alloys, *Earth Planet. Sci. Lett. 373*, 169-178.

Nakagawa, T. (2020) A coupled core-mantle evolution: review and future prospects, *Progress Earth Planet. Sci. 7*, 57, 2020.

Nakagawa, T. & Tackley, P.J. (2010) Influence of initial CMB temperature and other parameters on the thermal evolution of Earth's core resulting from thermochemical spherical mantle convection, *Geochem. Geophys. Geosystems 11*, Q06001.

Nakagawa, T. & Tackley, P.J. (2015) Influence of plate tectonic mode on the coupled thermochemical evolution of Earth's mantle and core, *Geochem. Geophys. Geosystems 16*, 3400-3413.

Nakajima, M. & Stevenson, D.J. (2015) Melting and mixing states of the Earth's mantle after the Moon-forming impact, *Earth Planet. Sci. Lett. 427,* 286-295.

Nakajima, Y., Imada, S., Hirose, K., Komabayashi, T., Ozawa, H., Tateno, S., Tsutsui, S., Kuwayama, Y., Baron, A.Q.R. (2015). Carbon-depleted outer core revealed by sound velocity measurements of liquid iron-carbon alloy, *Nature Commun. 6*, 8942.

Nakajima, Y., Kawaguchi, S.I., Hirose, K., Tateno, S., Kuwayama, Y., Sinmyo, R., Ozawa, H., Tsutsui, S., Uchiyama, H. & Baron, A.Q.R. (2020). Silicon-depleted present-day Earth's outer core revealed by sound velocity measurements of liquid Fe-Si alloy, *J. Geophys. Res. 125*, e2020JB019399.

Nimmo, F., (2015) Thermal and compositional evolution of the core, *Treatise Geophys. Vol. 9,* 201-219.

Nimmo, F., & Kleine, T. (2015) Early Differentiation and core formation: processes and timescales, in Early Earth: Accretion and differentiation, *Geophys. Mongr. Book Ser. 212*, 83-102.

Nimmo, F., Primack, J., Faber, S.M., Ramirez-Ruiz, E. & Safarzadeh, M. (2020) Radiogenic heating and its influence on rocky planet dynamos and habitability, *Astrophys. J. Lett. 903*, L37.

O'Brien, D.P., Walsh, K.J, Morbidelli, A., Raymond, S.N. & Mandell, A.M. (2014) Water delivery and giant impacts in the Grand Tack scenario, *Icarus 239*, 74-84.

Ohta, K., Kuwayama, Y., Hirose, K., Shimizu, K., & Ohishi, Y. (2016) Experimental determination of the electrical resistivity of iron at Earth's core conditions, *Nature 534,* 95-98.

Olson, P. (2016) Mantle control of the geodynamo: Consequences of top-down regulation, *Geochem. Geophys. Geosystems 17*, 1935-1956.

Olson, P. & Sharp, Z.D. (2019) Nebular atmosphere to magma ocean: A model for volatile capture during Earth accretion, *Phys. Earth Planet. Inter. 294*, 106294.

Ozawa, H., Hirose, K., Tateno, S., Sata, N. & Ohishi, Y. (2010) Phase transition boundary between B1 and B8 structures of FeO up to 210 GPa, *Phys. Earth Planet. Inter. 179*, 157-163.

Poirier, J.P. (1994) Light elements in the Earth's outer core- a critical review, *Phys. Earth Planet. Inter. 85*, 319-337.

Pozzo, M., Davies, C., Gubbins, D. & Alfe, D. (2012) Thermal and electrical conductivity of iron at Earth's core conditions, *Nature 485,* 355-358.

Raymond, S.N., Quinn, T. & Lunine, J.I. (2006) High-resolution simulations of the final assembly of Earth-like planets 1. Terrestrial accretion and dynamics, *Icarus 183*, 265-282.

Ringwood, A.E. (1977) Composition of core and implications for origin of Earth, *Geochem. J.* 11, 111-135.

Rubie, D.C., Melosh, H.J., Reid, J.E., Liebske, C. & Righter, K. (2003) Mechanisms of metal-silicate equilibration in the terrestrial magma ocean, *Earth Planet. Sci. Lett. 205*, 239-255.

Rubie, D.C., Frost, D.J., Mann, U., Asahara, Y., Nimmo, F., Tsuno, K., Kegler, P., Holzheid, A. & Palme, H. (2011) Heterogeneous accretion, composition and core-mantle differentiation of the Earth, *Earth Planet. Sci. Lett. 301*, 31-42.

Rubie, D.C., F. Nimmo, H.J. Melosh (2015a), Formation of the Earth's core, *Treatise Geophys. Vol. 8*, 27-55.

Rubie D.C., Jacobson, S.A., Morbidelli, A., O'Brien, D.P., Young, E.D., de Vries, J., Nimmo, F., Palme, H. & Frost, D.J. (2015b) Accretion and differentiation of the terrestrial planets with implications for the compositions of early-formed Solar System bodies and accretion of water, *Icarus 248*, 89-108.

Rudge, J.F., Kleine, T., & Bourdon, B. (2010) Broad bounds on Earth's accretion and core formation constrained by geochemical models, *Nature Geosci. 3*, 439-443.

Schonbachler, M., Carlson, R.W., Horan, M.F., Mock, T.D. & Hauri, E.H. (2010) Heterogeneous accretion and the moderately volatile element budget of Earth *Science 328,* 884-887.

Shi, C.Y., Zhang, L., Yang, W.G., Liu, Y.J., Wang, J.Y., Meng, Y., Andres, J.C. & Mao, W.L. (2013) Formation of an interconnected network of iron melt at Earth's lower mantle conditions, *Nature Geosci. 6,* 971-975.

Siebert, J., Badro, J., Antonangeli, D., & Ryerson, F.J. (2013) Terrestrial accretion under oxidizing conditions, *Science 339*, 1194-1197.

Stacey, F.D. & Anderson, O.L. (2001) Electrical and thermal conductivities of Fe-Ni-Si alloy under core conditions, *Phys. Earth Planet. Inter. 124*, 153-162.

Suer, T.A., Siebert, J., Remusat, L., Menguy, N. & Fiquet, G. (2017) A sulfur-poor terrestrial core inferred from metal-silicate partitioning experiments, *Earth Planet. Sci. Lett*. 469, 84-97.

Tsuno, K., Frost, D.J., Rubie, D.C. (2013) Simultaneous partitioning of silicon and oxygen into the Earth's core during early Earth differentiation, *Geophys. Res. Lett*. 40, 66-71.

Yuan, L. & Steinle-Neumann, G. (2020) Strong sequestration of hydrogen into the Earth's core during planetary differentiation, *Geophys. Res. Lett. 47*, e2020GL088303.

Stevenson, D.J. (1990) Fluid dynamics of core formation, in Newsom, H.E. & Jones, J.H., Origin of the Earth, Oxford Univ. Press.

Tagawa, S., Ohta, K., Hirose, K., Kato, C., & Ohishi, Y. (2016) Compression of Fe-Si-H alloys to core pressures, *Geophys. Res. Lett. 43*, 3686-3692.

Tarduno, J.A., Cottrell, R.D., Bono, R.K. et al., (2020) Paloemagnetism indicates that primary magnetite in zircon records a strong Hadean geodynamo, *Proc. Nat. Acad. Sci. USA, 117*, 2309-2318.

Umemoto, K. & Hirose, K. (2020) Chemical compositions of the outer core examined by first principles calculations, *Earth Planet. Sci. Lett. 531*, 116009.

Walsh, K.J., Morbidelli, A., Raymond, S.N., O'Brien, D.P. & Mandell, A.M. (2011) A low mass for Mars from Jupiter's early gas-driven migration. *Nature 475*, 206-209.

Wang, H.P., Weiss, B.P., Bai, X.N. et al. (2017) Lifetime of the solar nebula constrained by meteorite paleomagnetism, *Science 355*, 623-625.

Williams, Q. (2018) The thermal conductivity of Earth's core: A key geophysical parameter's constraints and uncertainties, *Ann. Rev. Earth Planet. Sci. 46*, 47-66.

Wu, B., Driscoll, P., Olson, P. (2011) A statistical boundary layer model for the mantle D” region, *J. Geophys. Res. 116*, B12112.

Xiong, Z., Tsuchiya, T. & Taniuchi, T. (2018) Ab initio prediction of potassium partitioning into Earth’s core, *J. Geophys. Res. 123*, 6451-6458.

Xu, J.Q., Zhang, P., Haule, K., Minar, J., Wimmer, S., Ebert, H. & Cohen, R.E. (2018) Thermal conductivity and electrical resistivity of solid iron at Earth’s core conditions from first principles, *Phys. Rev. Lett. 121*, 096601.

Yoshino, T., Walter, M.J., Katsura, T. (2003) Core formation in planetesimals triggered by permeable flow, *Nature 422,* 154-157.

Zhang, Y.J., Sekine, T., He, H.L., Yu, Y., Liu, F.S. & Zhang, M.J. (2016) Experimental constraints on light elements in the Earth’s outer core, *Scientific Reports 6*, 22473.

Zhang, Y.J., Hou, M.W., Liu, G.T., Zhang, C.W., Prakapenka, V.B., Greenberg, E., Fei, Y.W., Cohen, R.E. & Lin, J.F. (2020) Reconciliation of experiments and theory on transport properties of iron and the geodynamo, *Phys. Rev. Lett. 125*, 078501.

Zou, Z., Koper, K.D., Cormier, V.F. (2008) The structure of the base of the outer ore inferred from seismic waves diffracted around the inner core, *J. Geophys. Res. 113*, B05314.

Zube, N.G., Nimmo, F., Fischer, R.A., & Jacobson, S.A. (2019) Constraints on terrestrial planet formation timescales and equilibration processes in the Grand Tack scenario from Hf-W isotopic evolution, *Earth Planet. Sci. Lett. 522*, 210-218.

Further Reading

Hirose, K., Labrosse, S. & Hernlund, J. (2013) Composition and state of the core, *Ann. Rev. Earth Planet. Sci. 41*, 657.

Litasov, K.D. & Shatskiy, A.F. (2016) Composition of the Earth’s core: A review, *Russian Geol. Geophys. 57*, 22-46.

McDonough, W.F. (2003) Compositional model for the Earth’s core, *Treatise Geochem. Vol. 2*, p.547-568

Nakagawa, T. (2020) A coupled core-mantle evolution: review and future prospects, *Progress Earth Planet. Sci. 7*, 57, 2020.

Nimmo, F., (2015) Thermal and compositional evolution of the core, *Treatise Geophys. Vol. 9,* 201-219.

Nimmo, F., & Kleine, T. (2015) Early Differentiation and core formation: processes and timescales, in Early Earth: Accretion and differentiation, *Geophys. Mongr. Book Ser. 212*, 83-102.

Rubie, D.C., F. Nimmo, H.J. Melosh (2015a), Formation of the Earth's core, *Treatise Geophys. Vol. 8*, 27-55.

Stevenson, D.J. (1990) Fluid dynamics of core formation, in Newsom, H.E. & Jones, J.H., Origin of the Earth, Oxford Univ. Press.

Poirier, J.P. (1994) Light elements in the Earth's outer core- a critical review, *Phys. Earth Planet. Inter. 85*, 319-337.

Williams, Q. (2018) The thermal conductivity of Earth's core: A key geophysical parameter's constraints and uncertainties, *Ann. Rev. Earth Planet. Sci. 46*, 47-66.